Supporting Information

Reduced graphene oxide aerogel membranes through hydrogen bond mediation for highly efficient oil/water separation

*Mingrui He†, Runnan Zhang†, Kan Zhang, Yanan Liu, Yanlei Su and Zhongyi Jiang**

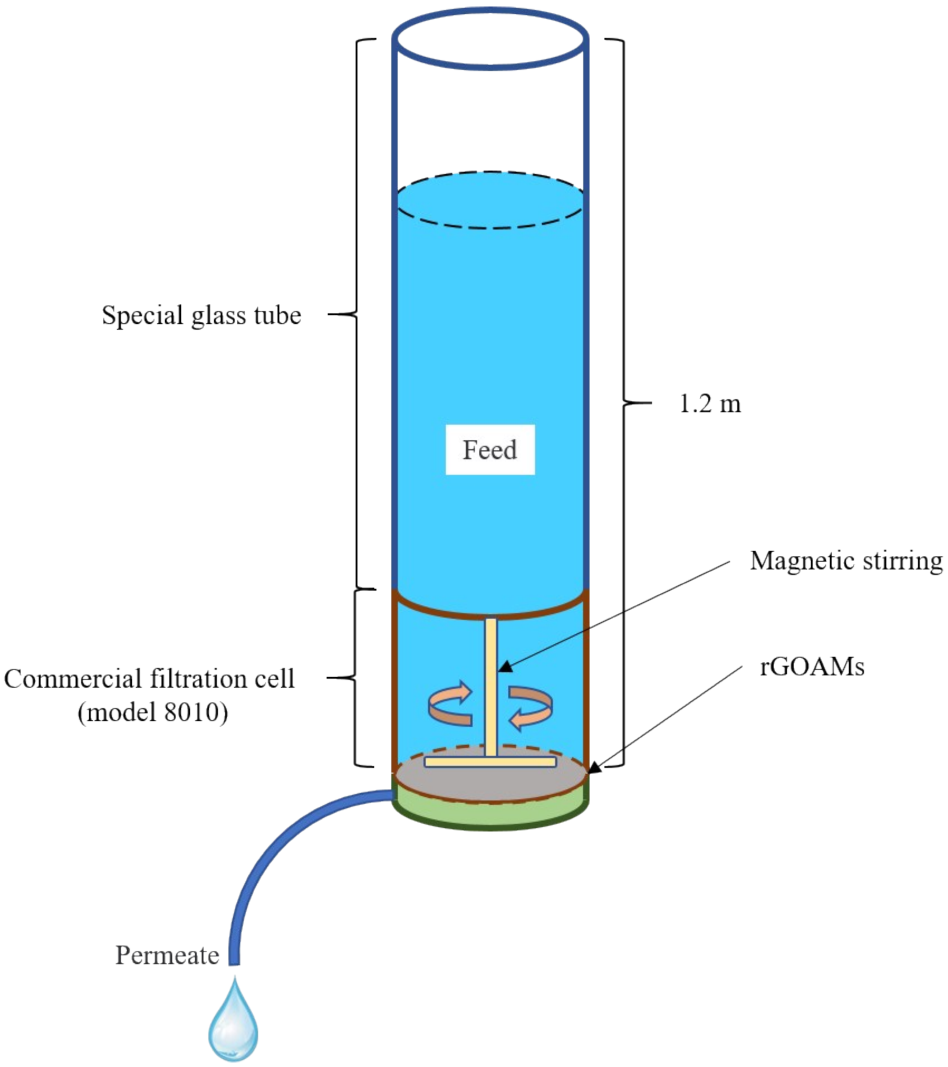

Fig. S1 Schematic illustration of the gravity-driven dead-end stirred cell filtration system.

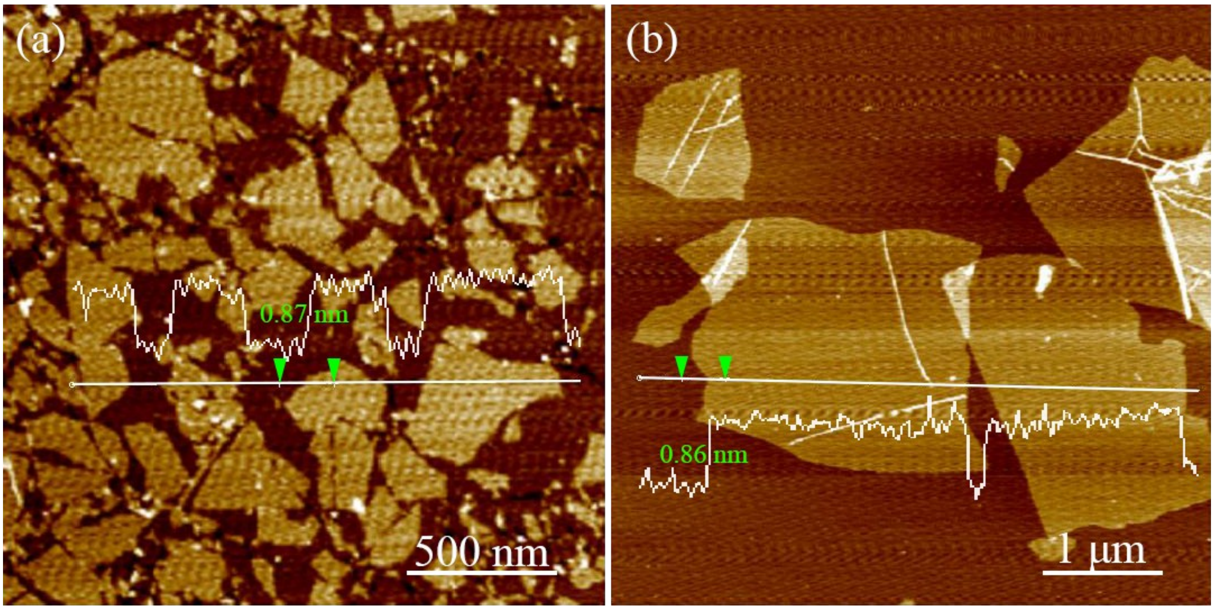

Fig. S2. AFM morphology of initial monolayer GO nanosheets with the theoretical average size of (a) 300 nm and (b) 3 μm.

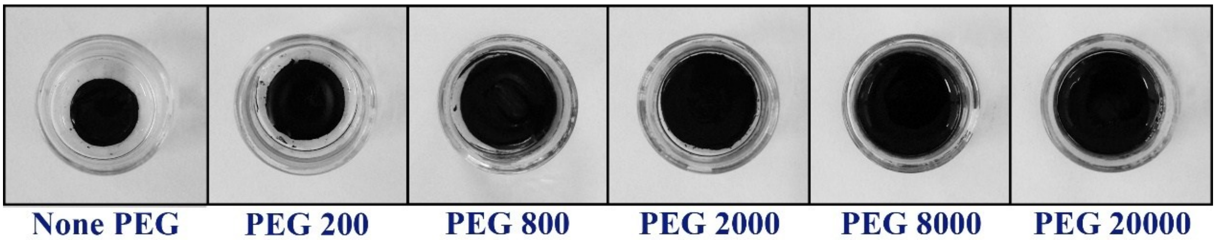

Fig. S3. Macroscopic profiles of the pure rGOAM and PEG-rGOAMs with Mw_{PEG} from 200 to 20000 Da prepared in cylindrical molds with the diameter of 2.5.

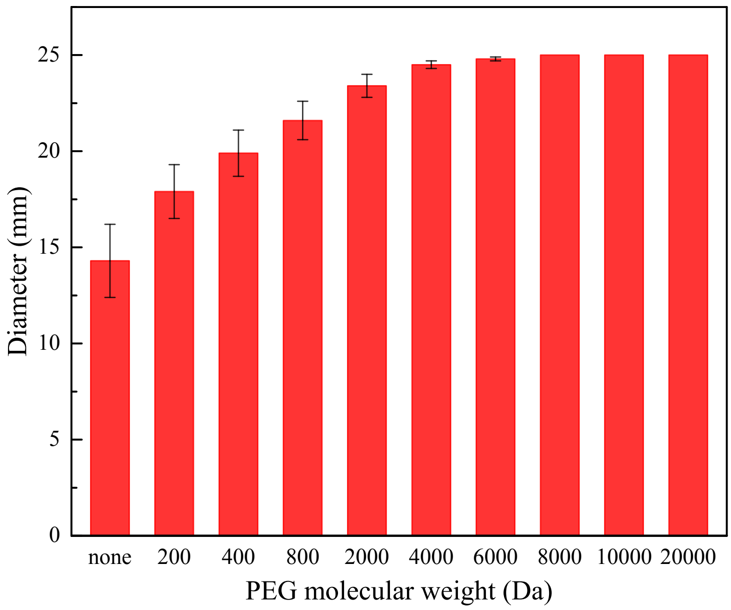

Fig. S4. Diameter of the pure rGOAM and PEG-rGOAMs with Mw_{PEG} from 200 to 20000 Da prepared in the cylindrical mold with the diameter of 25.0 mm.

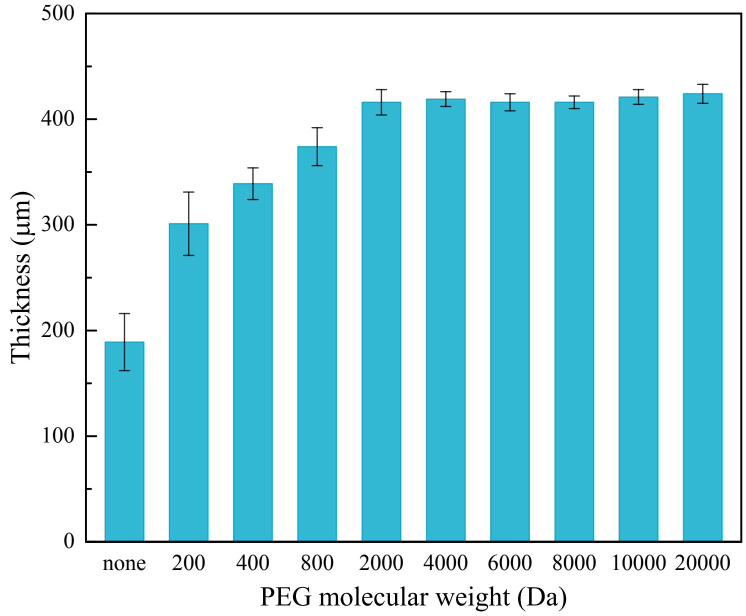

Fig. S5. Thickness of the pure rGOAM and PEG-rGOAMs with Mw_{PEG} from 200 to 20000 Da prepared in the cylindrical mold with the diameter of 50.0 mm.

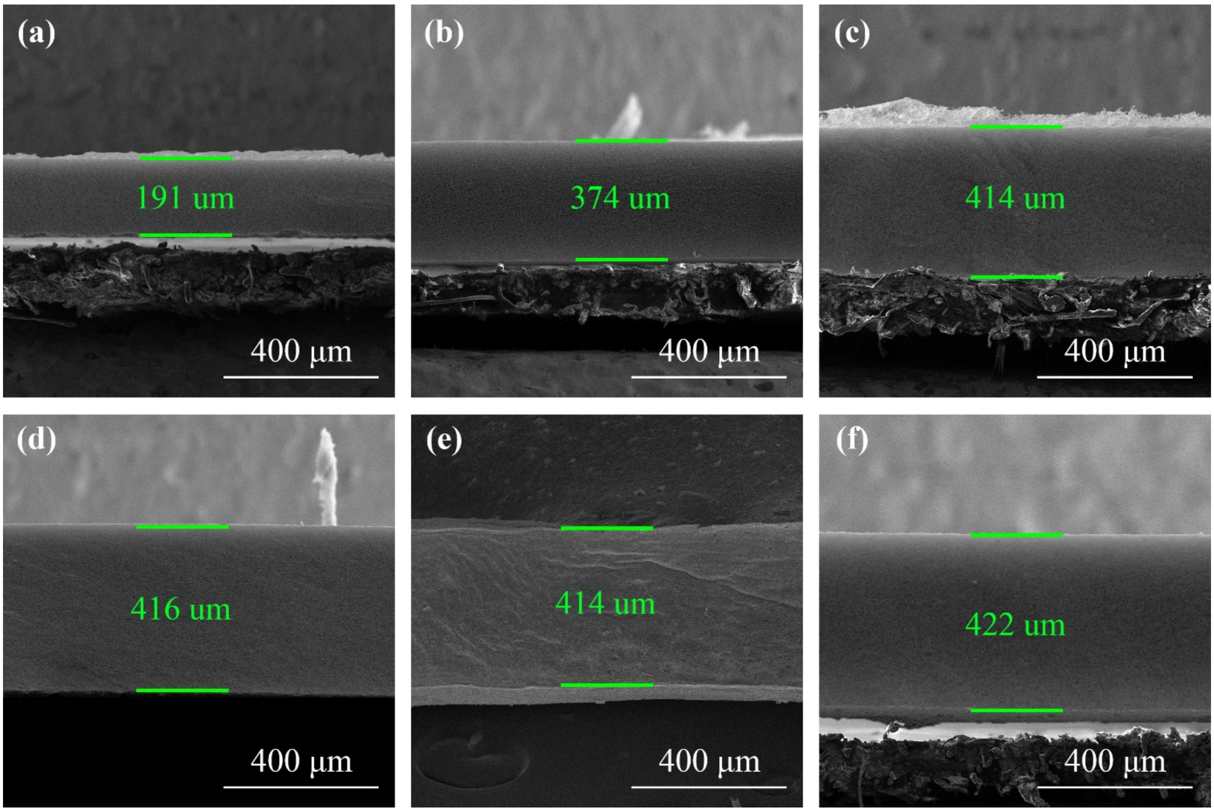

Fig. S6 Cross-sectional SEM images of (a) the pure rGOAM and PEG-rGOAMs with Mw_{PEG} of (b) 200, (c) 800, (d) 2000, (e) 8000, (f) 20000 Da.

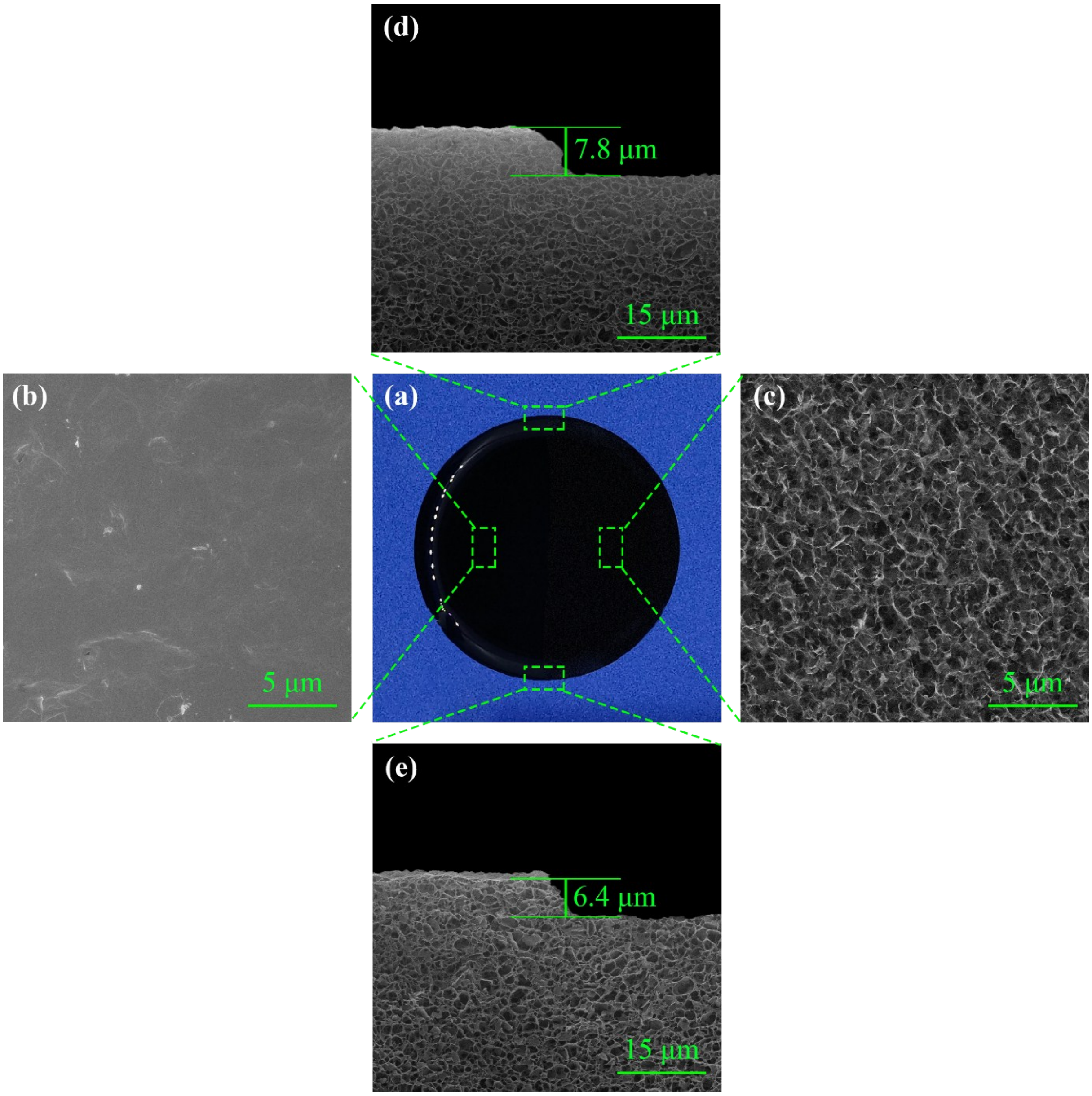

Fig. S7 (a) Photographic image of the virgin PEG-rGOAM (Mw_{PEG} of 8000) with the right half of the surface treated by metallographic abrasive paper (P2000). Surface morphology of the PEG-rGOAM (b) before and (c) after treatment. (e) and (f) Cross-sectional SEM images of the boundary, showing the thickness of the removed dense surrface layer.

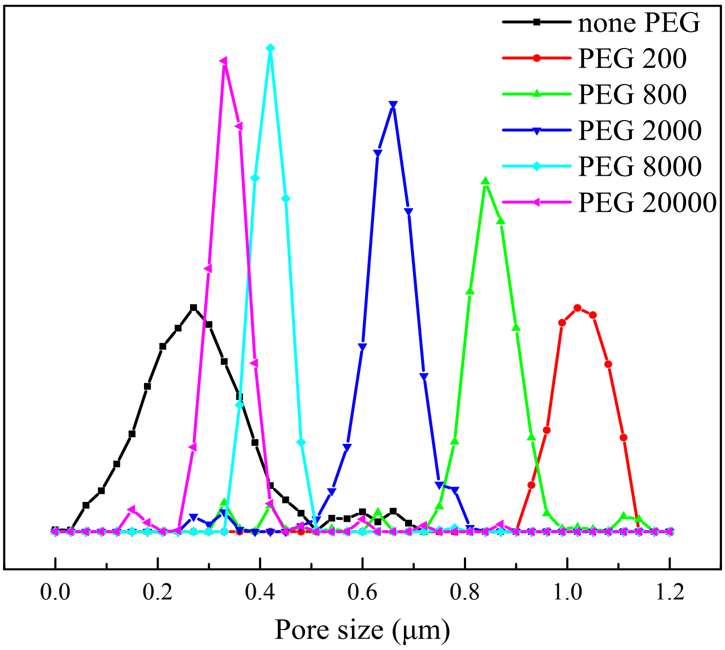

Fig. S8. Pore size distribution of the pure rGOAM and PEG-rGOAMs with Mw_{PEG} from 200 to 20000 Da acquired by the bubble-pressure method.

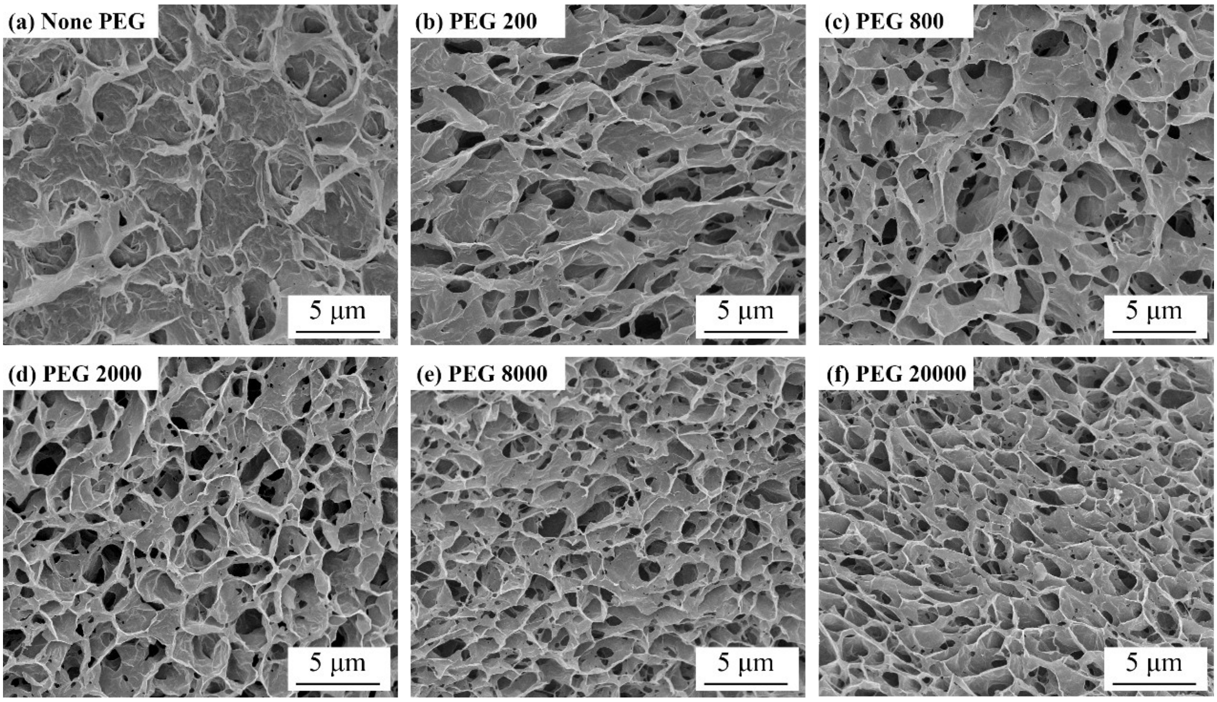

Figure S9. Surface morphology of the pure rGOAM and PEG-rGOAMs with Mw_{PEG} from 200 to 20000 Da prepared with large initial GO nanosheets (theoretical average size = 3 μm).

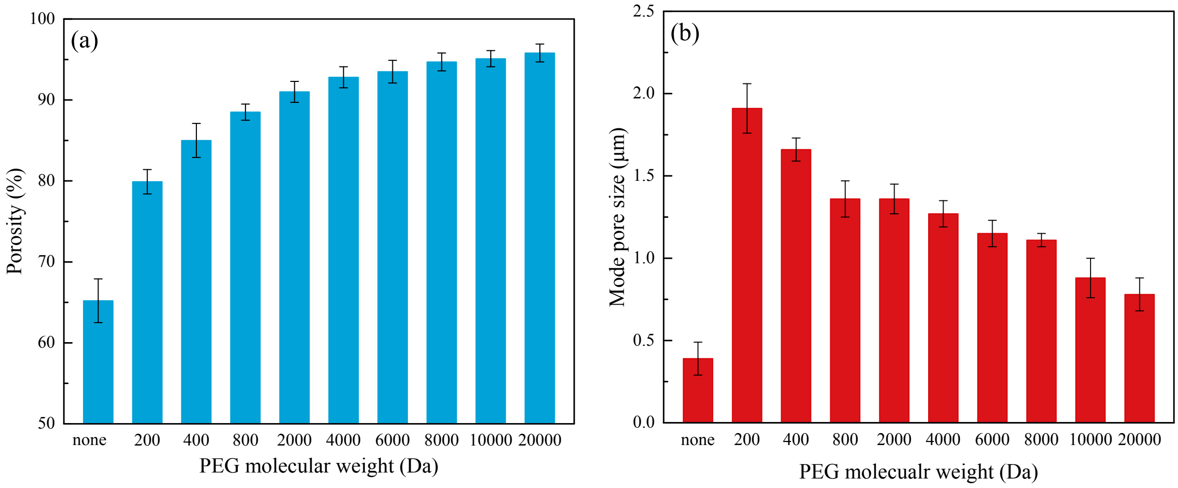

Figure S10. (a) Porosity and (b) mean pore sizes of the pure rGOAMs and PEG-rGOAMs with Mw_{PEG} from 200 to 20000 Da prepared with large initial GO nanosheets (theoretical average size = 3 μm).

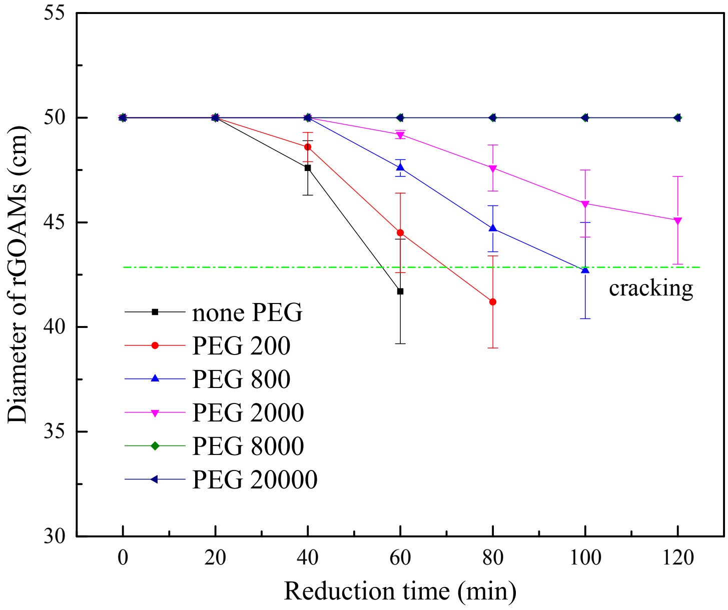

Figure S11. Reduction time-dependent diameter of the pure rGOAM and PEG-rGOAMs with Mw_{PEG} from 200 to 20000 Da.

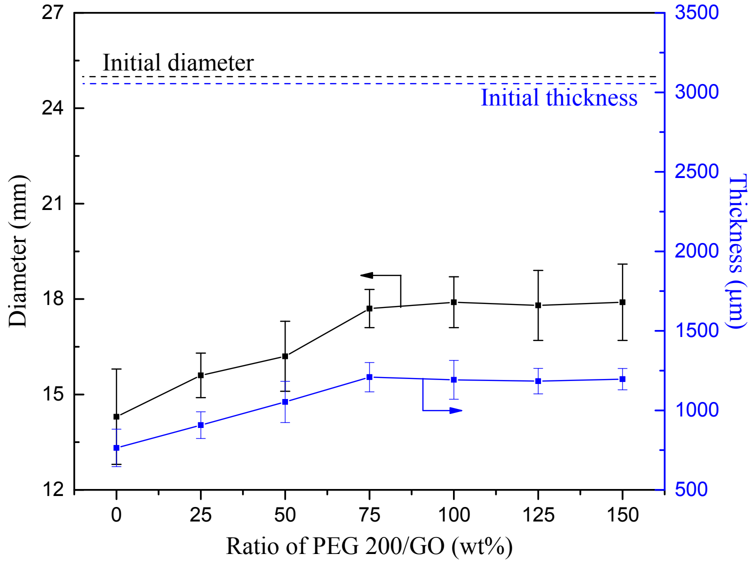

Figure S12. Diameter and thickness of the pure rGOAM and PEG-rGOAMs with the mass ratios of PEG 200/GO from 25wt% to 150wt%.

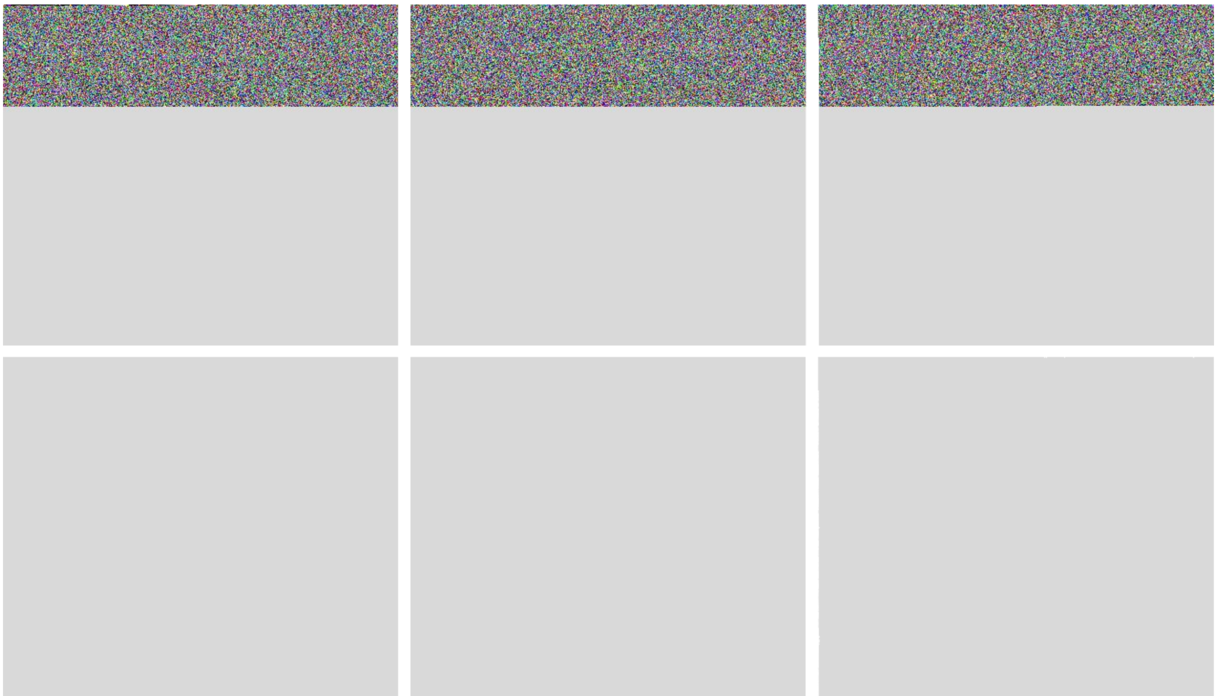

Figure S13. Surface morphology of the pure rGOAM and PEG-rGOAMs with the mass ratios of PEG 200/GO from 25wt% to 150wt%.

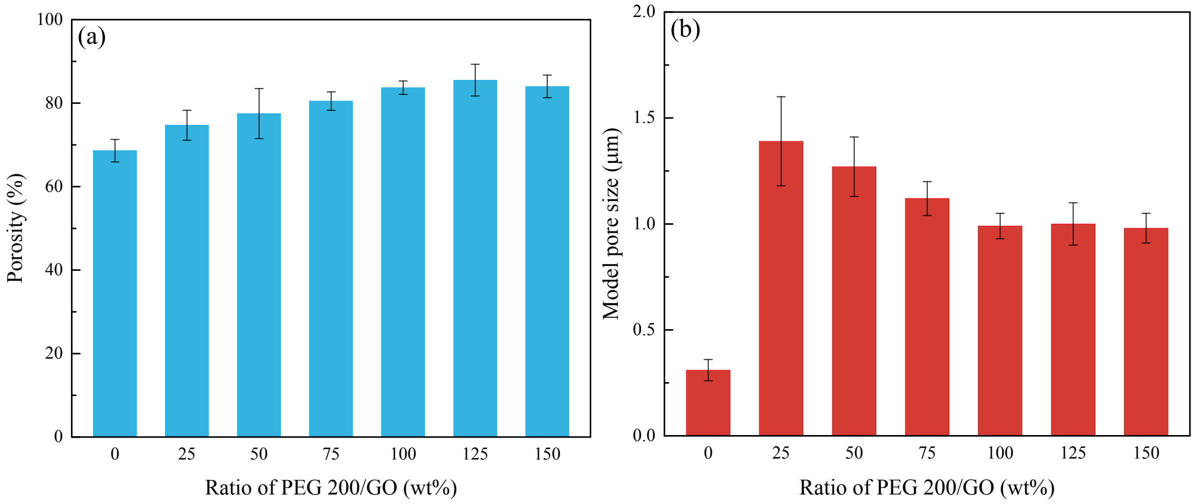

Figure S14. (a) Porosity and (b) mean pore sizes of the pure rGOAM and PEG-rGOAMs with the mass ratios of PEG 200/GO from 25 wt% to 150 wt%.

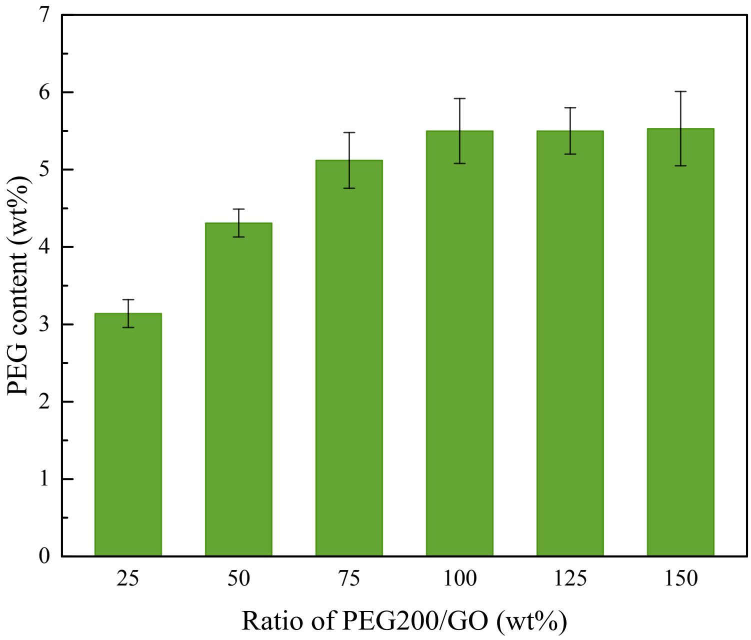

Figure S15. PEG contents in PEG-rGOAMs with the mass ratios of PEG 200/GO from 0wt% to 150wt%.

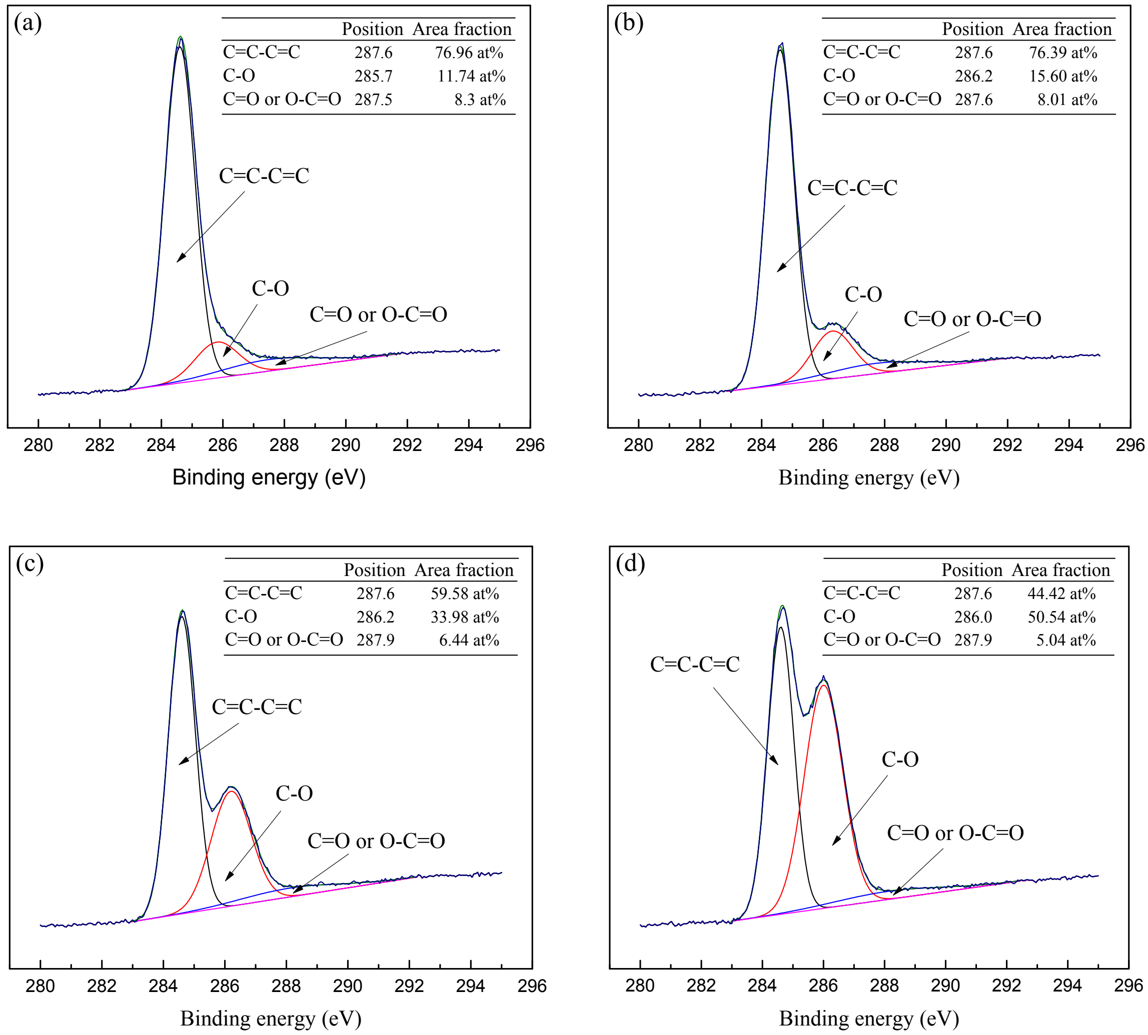

Figure S16. XPS C1s core level spectra of (a) the pure rGOAMs and PEG-rGOAMs with Mw_{PEG} of (b) 200, (c) 2000 and (d) 20000 Da.

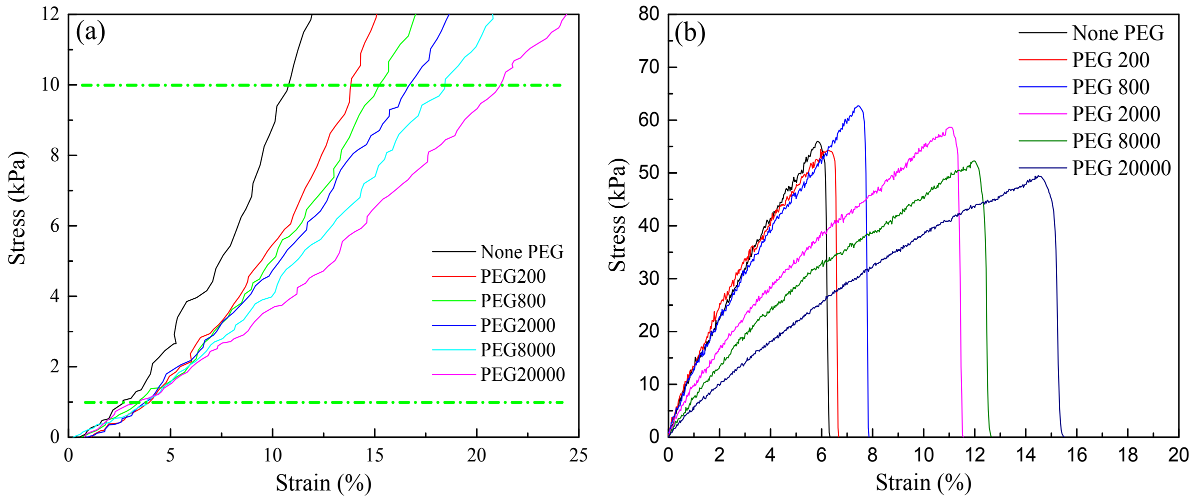

Figure S17. Stress-strain curves of the pure rGOAM and PEG-rGOAMs with Mw_{PEG} from 200 to 20000 Da in (a) the compressing test and (b) the stretching test.

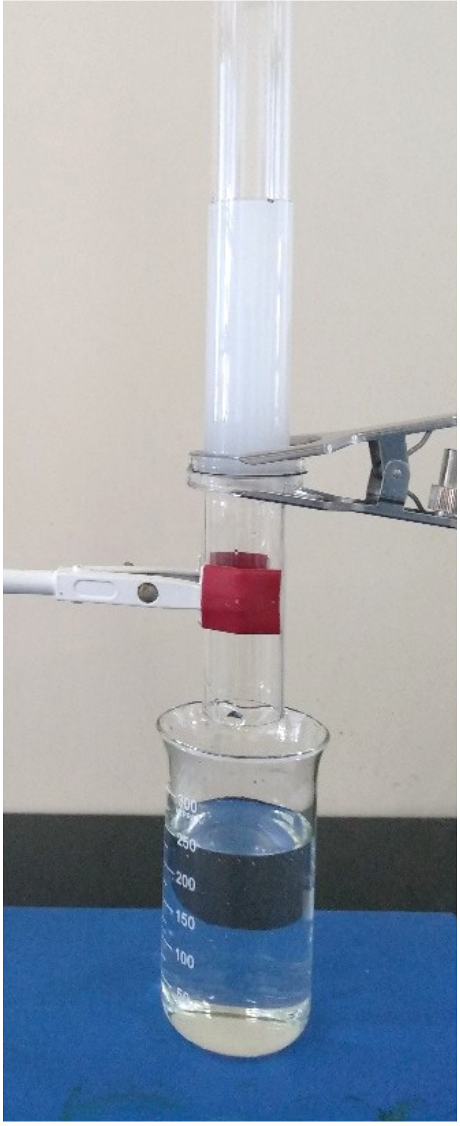

Figure S18. Photo of the PEG-rGOAM with Mw_{PEG} of 2000 Da utilized in the separation of corn oil-in-water emulsion.

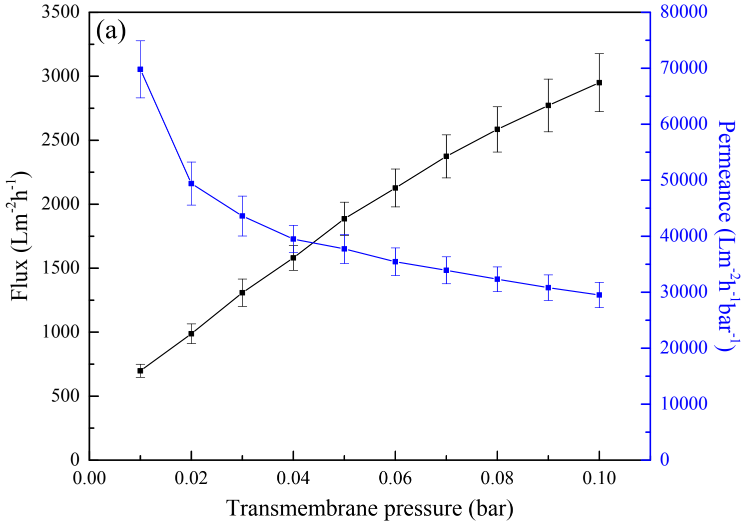

Figure S19. Flux and permeance of PEG-rGOAMs with Mw_{PEG} of 8000 Da under the transmembrane pressure varied from 0.01 bar to 0.1 bar.

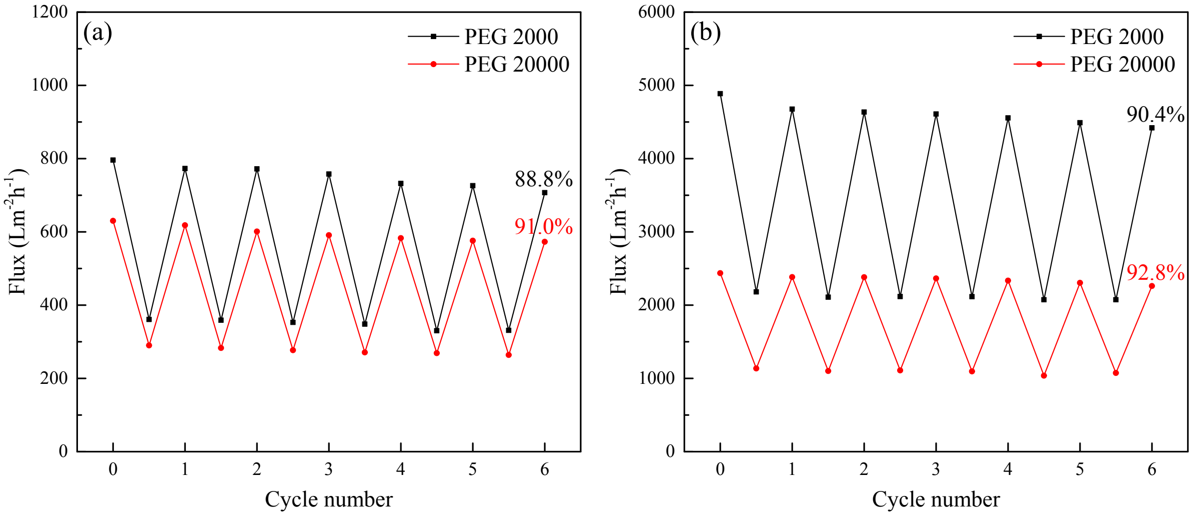

Figure S20. Antifouling performance of PEG-rGOAMs with Mw_{PEG} of 2000 and 20000 Da in the separation of corn oil-in-water emulsion under the pressure of (a) 0.01 and (b) 0.1 bar.

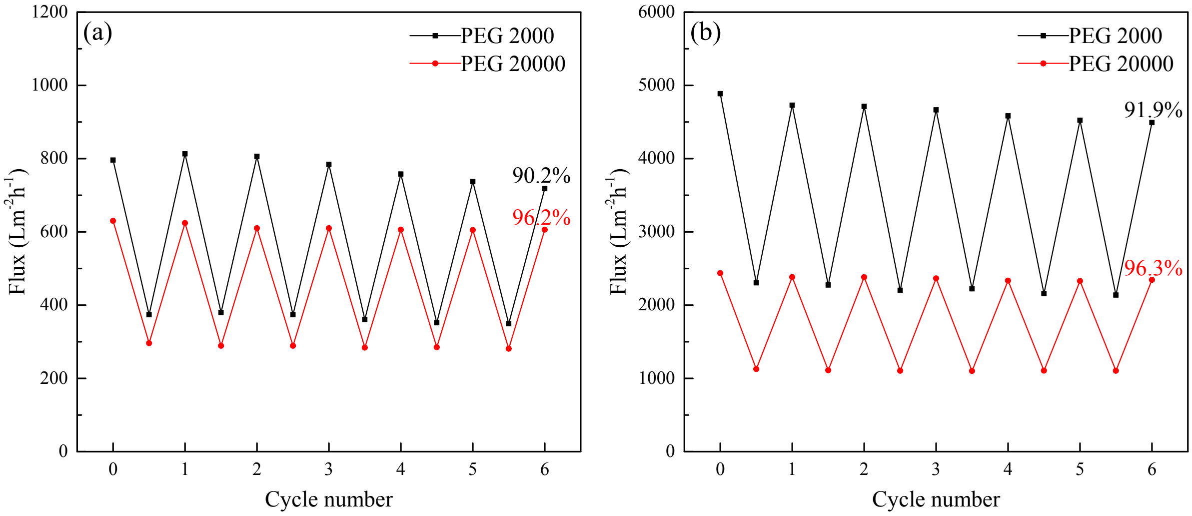

Figure S21. Antifouling performance of PEG-rGOAMs with Mw_{PEG} of 2000 and 20000 Da in the separation of bump oil-in-water emulsion under the pressure of (a) 0.01 and (b) 0.1 bar.

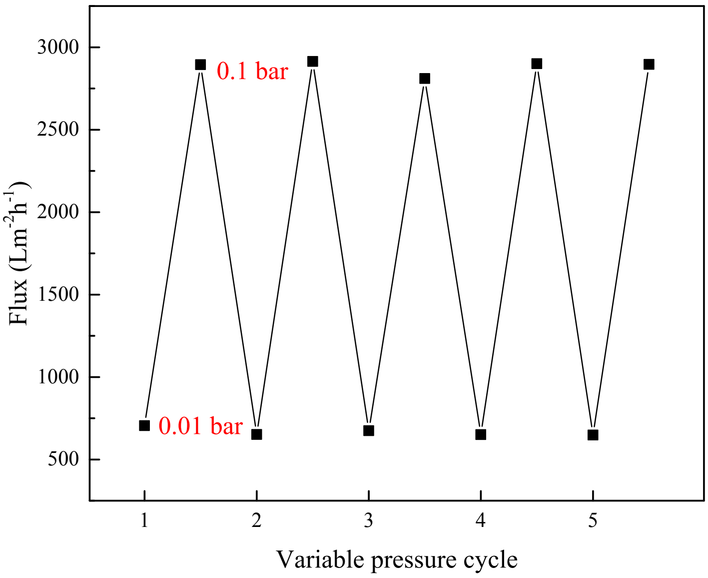

Figure S22. Operational stability of the PEG-rGOAM with Mw_{PEG} of 8000 Da in the variable pressure cycling test.

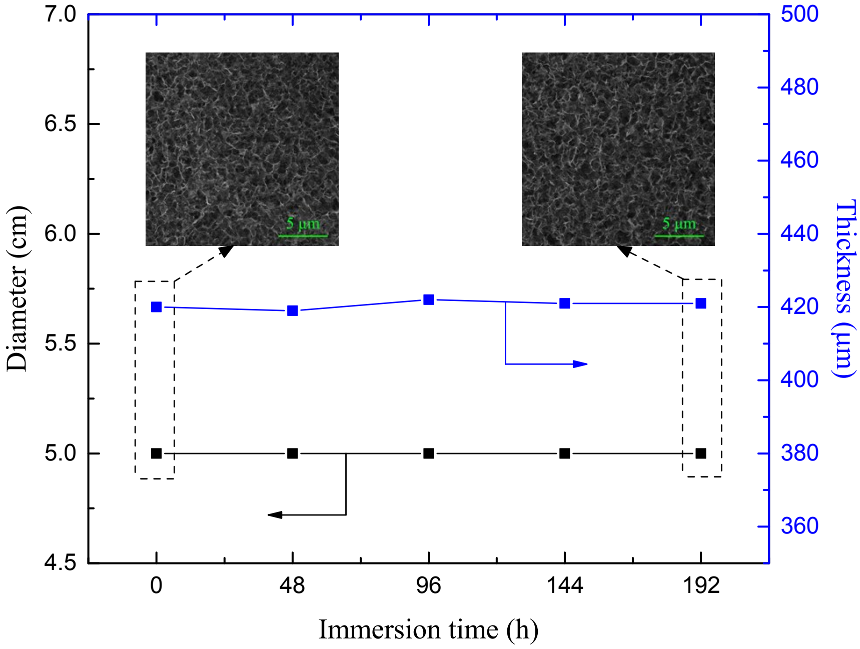

Fig. S23. The morphology of the PEG-rGOAM with Mw_{PEG} of 2000 during the long-term immersing test.

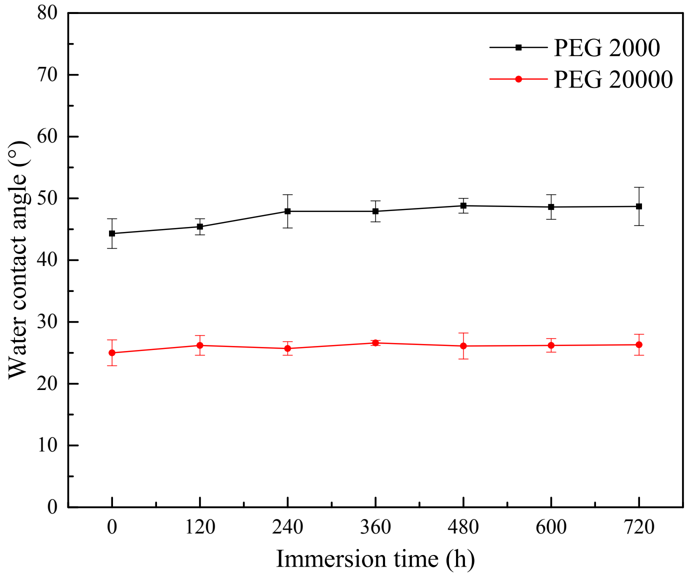

Figure S24.The surface water contact angles of PEG-rGOAMs with Mw_{PEG} of 2000 and 20000 Da during the immersing test.

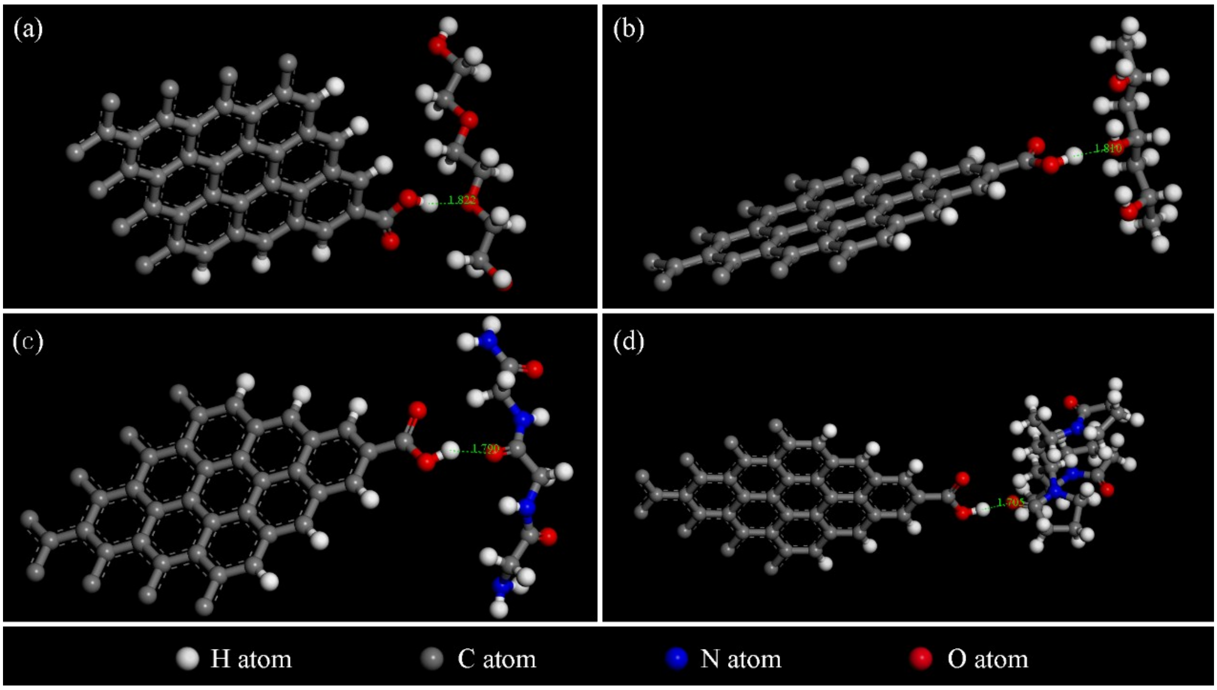

Figure S25. Calculation of the hydrogen bond length of the polymers with benzoic carboxyl groups of rGO nanosheets in the (a) PEG-rGOAM, (b) PVA-rGOAM, (c) polyglycine-rGOAM and (d) PVP-rGOAM by Materials Studio.

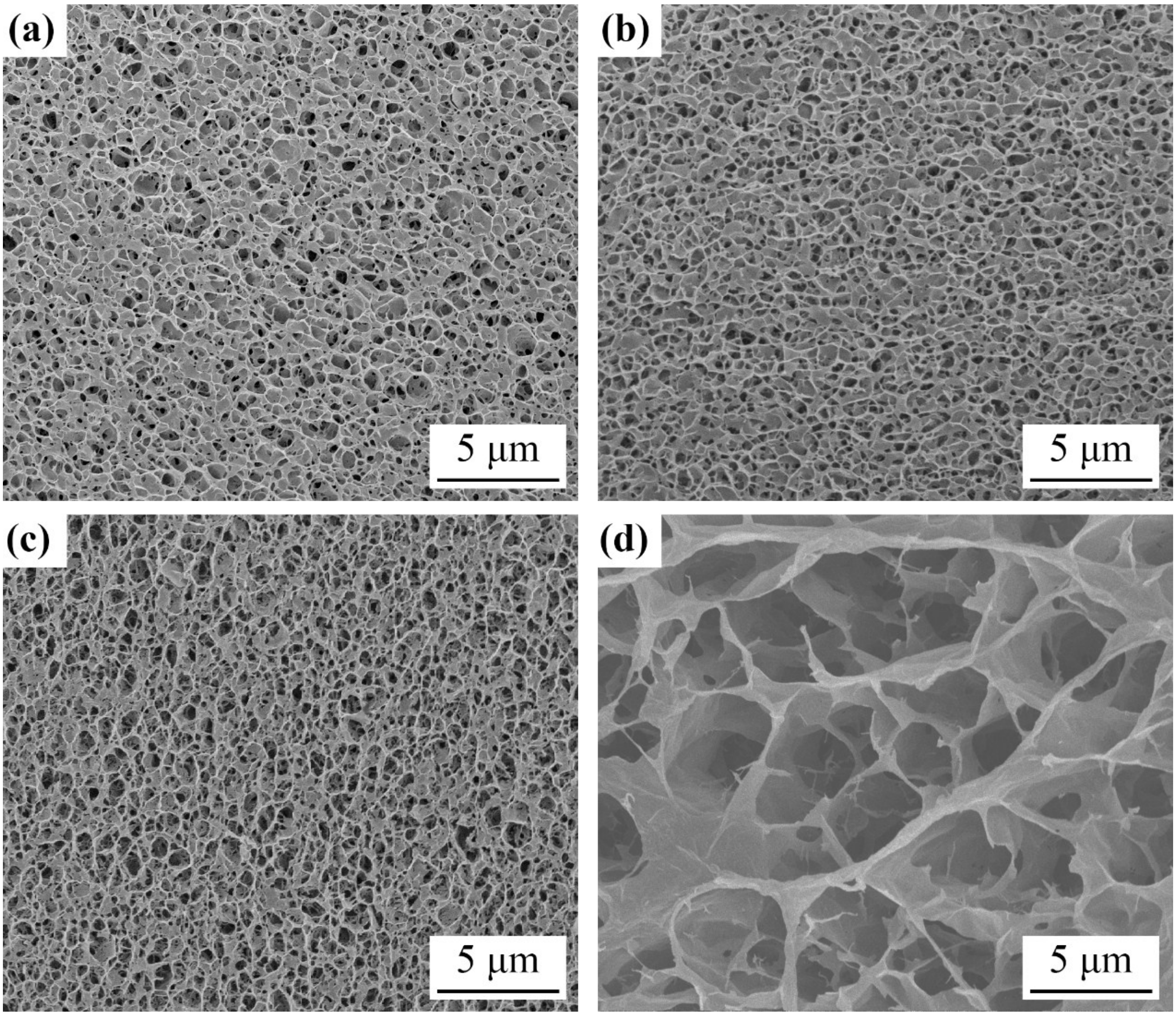

Figure S26. Surface morphology of the (a) PEG-rGOAM, (b) PVA-rGOAM, (c) polyglycine-rGOAM and (d) PVP-rGOAM.

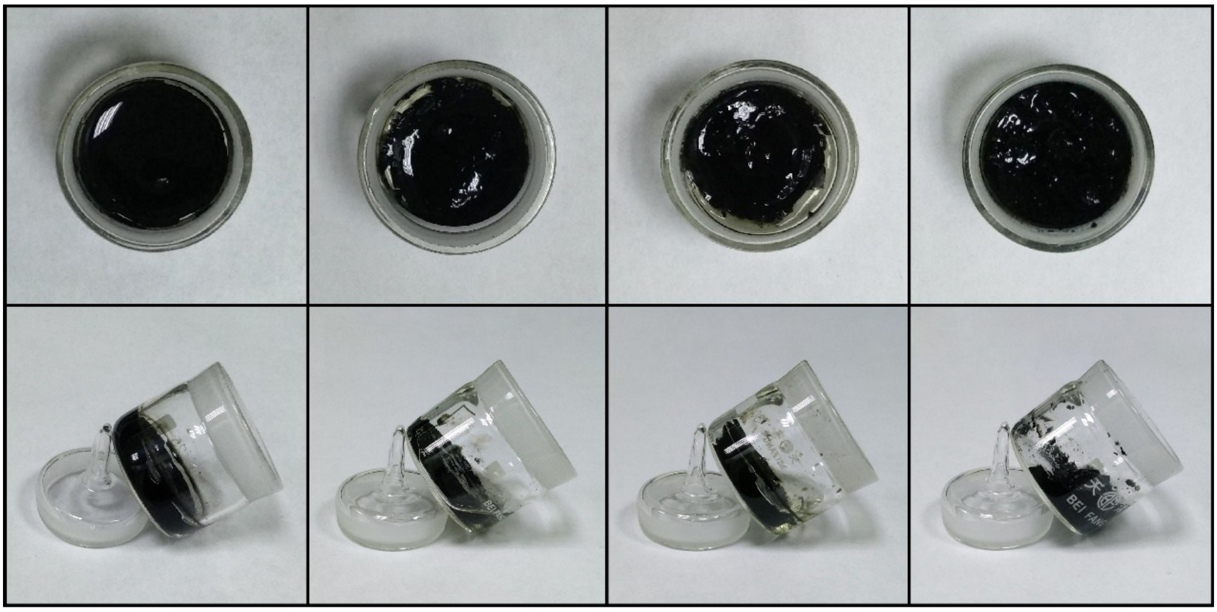

PEG **PVA** **polyglycine** **PVP**

Figure S27. Macroscopic profiles and membrane-forming properties of PEG-rGOAM, PVA-rGOAM, polyglycine-rGOAM and PVP-rGOAM.

Table S1 Performance comparison of GO-based membranes for oil-in-water separation

Assembly structure	Membrane	Pore sizes (nm)	Operating pressure (bar)	Flux ($Lm^{-2}h^{-1}$)	Oil droplet sizes	Rejection	Reference
3D	rGOAMs/PEG 20000	330	0.10	2830	370 nm	nearly 100%	this work
	rGOAMs/PEG 2000	620	0.10	4890	920 nm	nearly 100%	this work
	GOAM/alginate/Ca^+	more than 50000	0.016	13680	dispersed oil	about 99%	1
	GOAM/PEI	N.A.	0.012	600	emulsified oil	more than 99.5%	2
2D	GO/palygorskite	1.13	0.50	1867	210 nm	more than 99.9%	3
	GO/g-C_3N_4/TiO_2	1.96	0.50	2270	200 nm	more than 99.9%	4
	GO/dopamine	N.A.	about 1.0	about 3000	70 nm	about 99.6%	5
	GO/PDA-HNTs	N.A.	0.9	630	170 nm	99.5%	6
	GO/PDA/MCEM	0.85	0.9	80	emulsified oil	96%	7

1. Y. Li, H. Zhang, M. Fan, P. Zheng, J. Zhuang and L. Chen, *Scientific Reports*, 2017, 7.
2. T. Huang, L. Zhang, H. Chen and C. Gao, *Journal of Materials Chemistry A*, 2015, 3, 19517-19524.
3. X. Zhao, Y. Su, Y. Liu, Y. Lip and Z. Jiang, *Acs Applied Materials & Interfaces*, 2016, 8, 8247-8256.
4. Y. Liu, Y. Su, J. Guan, J. Cao, R. Zhang, M. He, K. Gao, L. Zhou and Z. Jiang, *Advanced Functional Materials*, 2018, 28.
5. N. Liu, M. Zhang, W. Zhang, Y. Cao, Y. Chen, X. Lin, L. Xu, C. Li, L. Feng and Y. Wei, *Journal of Materials Chemistry A*, 2015, 3, 20113-20117.
6. Y. Zhan, S. He, X. Wan, S. Zhao and Y. Bai, *Journal of Membrane Science*, 2018, 567, 76-88.
7. Z. Liu, W. Wu, Y. Liu, C. Qin, M. Meng, Y. Jiang, J. Qiu and J. Peng, *Separation and Purification Technology*, 2018, 199, 37-46.